Voltage Frequency Control using SVC Devices coupled with Voltage Dependent Loads

Yong Wan, Mohammed Ahsan Adib Murad, *Student Member, IEEE*, Muyang Liu, *Student Member, IEEE*, and Federico Milano, *Fellow, IEEE*

***Abstract*—This paper proposes a decentralized control based on SVC devices to improve the frequency control of high voltage transmission systems. For a realistic structure preserving power system with voltage dependent loads, we propose a sufficient condition based on a strict Lyapunov energy function which is utilized to design a nonlinear adaptive SVC controller. This controller only requires local bus measures and parameters. Furthermore, we also present an SVC with a conventional frequency droop controller. The performance of the two considered SVC control systems are evaluated on the well-known IEEE New England 39-bus 10-machine power system and compared with conventional SVC controllers.**

***Index Terms*—Multi-machine power systems, voltage frequency control, structure preserving model, FACTS, decentralized control, Lyapunov function.**

NOMENCLATURE

VDL	Voltage Dependent Load
VFC	Voltage Frequency Control
SVC	Static Var Compensator
POD	Power Oscillation Damping
SLEF	Strict Lyapunov Energy Function
SPM	Structure Preserving Model
CSVC	Conventional Static Var Compensator
ASVC	Adaptive Static Var Compensator
DAE	Differential Algebraic Equation
COI	Center of Inertia
Z_0	Nominal value of any variable Z
ΔZ	Difference $\Delta Z = Z - Z_0$
$\dot{Z}$	Time derivative of any variable Z
∇_Z	First-order partial derivative $\nabla_Z = \frac{\partial}{\partial Z}$
∇_Z^2	Second-order partial derivative $\nabla_Z^2 = \frac{\partial^2}{\partial Z^2}$
$\mathrm{Hess}(\cdot)$	Hessian matrix of a function
m	Number of machines
b	Number of buses
$l, k, (j)$	Index of (machine) bus
Ω_l	Index set of buses which connect to bus l
$\bar{b}, (\bar{m})$	Index set of (machine) buses, $\bar{m} \subseteq \bar{b}$
V_{t_l}	Voltage magnitude at bus l, in pu
$\boldsymbol{V}$	Voltage magnitude column vector
θ_l	Voltage angle at bus l, in rad
$\boldsymbol{\theta}$	Voltage angle column vector
δ_j	Power angle of jth machine, in rad
$\boldsymbol{\delta}$	Power angle column vector
ω_j	Relative speed of jth machine, in pu
$\boldsymbol{\omega}$	Relative speed column vector
ω_{COI}	Frequency in COI frame, in pu
$\boldsymbol{z}$	Vector $\left[\boldsymbol{\delta}^{\mathrm{T}}\ \boldsymbol{\omega}^{\mathrm{T}}\ \boldsymbol{V}^{\mathrm{T}}\ \boldsymbol{\theta}^{\mathrm{T}}\right]^{\mathrm{T}}$
f_l	Frequency at bus l, in Hz
E'_{d_j}, E'_{q_j}	d- and q-axis stator transient voltages of jth machine, in pu
P_{e_j}, Q_{e_j}	Active and reactive powers generated by jth machine, in pu
$\boldsymbol{P_e}$	Active power column vector
P_{lk}, Q_{lk}	Active and reactive powers transmitted through the line between buses l and k, in pu
P_{L_l}, Q_{L_l}	Active and reactive powers consumed by the load at bus l, in pu

Yong Wan is with the College of Automation Engineering and the Jiangsu Key Laboratory of Internet of Things and Control Technologies, Nanjing University of Aeronautics and Astronautics, Nanjing, China. E-mail: wanyong@nuaa.edu.cn, wanyong17007@163.com

Mohammed Ahsan Adib Murad, Muyang Liu, and Federico Milano are with the School of Electrical and Electronic Engineering, University College Dublin, Ireland. E-mail: mohammed.murad@ucdconnect.ie, muyang.liu@ucdconnect.ie, federico.milano@ucd.ie

Yong Wan is supported by the National Natural Science Foundation of China, under Grant No. 61403194, and by the Natural Science Foundation of Jiangsu Province, under Grant No. BK20140836, and by China Scholarship Council, under Grant No. 201706835013.

Mohammed Ahsan Adib Murad, Muyang Liu, and Federico Milano are supported by Science Foundation Ireland under Grant No. SFI/15/IA/3074.

I. INTRODUCTION

A. Motivation

Due to environmental concerns, in recent years, the quota of renewable energy resources with respect to conventional synchronous power plants based on fossil fuels has steadily grown and reached significant penetration levels. This often results in low-inertia power systems, whose stability and control poses several challenges which are currently not fully resolved [1]–[3]. In this context, the frequency control through flexible loads, typically thermostatically controlled, is the most common strategy that has been considered on the demand side [4]–[6]. Frequency control through VDLs, on the other hand, has not been fully investigated so far. With this aim, we discuss VFC strategies through SVC devices.

B. Literature Review

As long as the power system will include synchronous generation, the frequency is an appropriate measure on the supply/demand balance and always required to be within operating range for stable and secure system operation. To control the frequency is thus a synonym of active power balance control. Balancing the power through voltage control is a less intuitive idea that nevertheless can contribute to the overall stability of the system [7].

VFC has been proposed in the literature based on the sensitivity of the reactive and active power of load to the changes in the voltage. Solutions that have been discussed in the literature consider load tap changer transformers (LTCTs) [8], [9] and automatic voltage regulators (AVRs) [10]. However, LTCT can only be utilized as a secondary and/or tertiary VFC because of its relatively slow behavior that is more appropriate for conservation voltage reduction [11]. On the other hand, AVRs require conventional synchronous generators and, thus, this approach is not expected to be effective in low-inertia systems.

Another possibility is to utilize FACTS devices. Due to the fact that FACTS do not provide active power support, only few attempts to study FACTS-based VFC have been proposed. Primary VFC is investigated by combining a storage in [12]. A VFC is proposed in [13] by including an additional feedback loop to an SVC that is installed at a synchronous generator bus. This kind of connection of SVCs, however, is very unlikely to happen in practice. Currently, this additional feedback loop, known as POD, is utilized for low frequency (0.1–2 Hz) oscillation damping [14], [15]. Finally, a fast smart transformer (FST) with VFC capability is discussed in [16]. FSTs, however, are not yet available in power systems. In the following, we focus exclusively on SVC devices, which are shunt connected devices and the most common and cheapest among FACTS devices.

C. VFC through Adaptive Tracking

In comparison with the previous VFC frameworks, we aim to propose faster/more flexible control method and simultaneously consider relative realistic VDLs, i.e., the load at each bus is modeled as *a voltage dependent function with an unknown parameter*. With this aim, FACTS such as SVC can provide us an opportunity to study VDL based Lyapunov function development (see Appendix B).

From a control system perspective, we have to ensure that the employed Lyapunov function is an SLEF. Reference [17] has identified that, as a fundamental limitation in constructing SLEF for SPM, active power demands are needed to be voltage-independent and must satisfy the usual constant power constraint. This partly limits the application of the Lyapunov method on SPM since some assumptions are needed to be made regarding loads and transmission lines etc. For example, references [17], [18] have constructed Lyapunov energy functions for the structure preserving power systems with constant active power load model.

In this paper, *we recast the SLEF construction problem of the SPM into the framework of tracking a desired signal.* We achieve this task by studying a nonlinear ASVC control strategy. Tracking control is a quite common problem in practice. For example, dynamic surface control has been proposed to guarantee boundedness of tracking error semi-globally, but it is not applicable if the first derivative of desired output trajectory is unknown [19]. Reference [20] has addressed the output feedback tracking problem by employing a dynamic compensator. However, this result needs prior information about the upper bound of the reference trajectory plus its derivative, which is also unavailable exactly. Thus, for the adaptive VFC, it is necessary to consider a more realistic load model with unknown parameters and the fact that the time derivative of the reference signal to be tracked is generally unavailable, and then to tackle the corresponding challenges.

D. Contribution

This paper proposes a nonlinear adaptive decentralized SVC control strategy for the SPM with VDLs to improve the frequency responses without deteriorating the voltage performances and an extended CSVC model by adding a lag VFC loop. Compared with previous work, the main features of the proposed framework are threefold:

- SVC-based VFC is studied.
- An adaptive control and a lag control for frequency stability enhancement considering VDLs are proposed, where only local measurements are needed.
- An adaptive scheme is proposed to maintain robustness of the SVC even though there exist uncertainties in the load model and the desired signal to be tracked.

E. Organization

The remainder of this paper is organized as follows: Section II describes the SVC model. Section III proposes a sufficient condition for SLEF, which relates to ASVC tracking control, and the challenges to be tackled. Then, the main theoretical results are presented and the proposed nonlinear adaptive decentralized SVC controller is designed. A case study based on the IEEE New England 39-bus 10-machine power system is discussed in Section IV. Conclusions are drawn in Section V.

II. SVC Modeling

SVC is a combination of variable shunt capacitor and reactor to maintain a constant voltage at the bus to which it is connected. The SVC model to be considered for adaptive frequency control design and the proposed extended CSVC model with lag frequency control loop are given in this section.

A. SVC Model for Adaptive VFC Design

We use the following first-order differential equation to represent an SVC at bus l:

$$T_{rl}\dot{b}_{rl} = -b_{rl} + u_l, \tag{1}$$

$$Q_{rl} = b_{rl}V_{t_l}^2, \tag{2}$$

where b_{rl} represents the susceptance of the SVC, in pu, T_{rl} is the time constant of the SVC model, in s, Q_{rl} is the output reactive power by the SVC, in pu, and u_l denotes the control variable to be designed later.

B. Extended CSVC Model

As depicted in Fig. 1, the CSVC model is represented as the following differential equation [21],

$$T_{rl}\dot{b}_{rl} = -b_{rl} + K_{rl}(V^{\text{ref}} - V_{t_l} + v_g), \tag{3}$$

$$Q_{rl} = b_{rl}V_{t_l}^2, \tag{4}$$

where V^{ref} denotes the reference voltage, K_{rl} is the constant gain, the additional signal v_g is designed by using lag control as follows,

$$T_g \dot{v}_g = -v_g + K_g \Delta f_l, \tag{5}$$

where T_g and K_g are the time constant and gain of the lag control respectively.

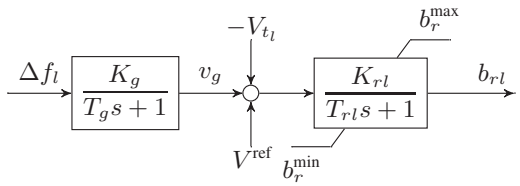

Fig. 1: Extended CSVC model: CSVC+VFC.

Note that, in the literature, v_g is generally obtained through a POD, which is sensitive only to the rate of change of the frequency. Instead, we model a lag control for which the input is the local bus frequency error, similar to what discussed in [13]. However, in [13], a proportional, integral and differential (PID) control loop is used to obtain v_g, and the SVC must be installed on a synchronous generator bus. Our proposed ASVC and extended CSVC do not have this limitation.

III. Main Results and SVC Control Design

In this section, we propose a sufficient condition for SLEF that has a unique minimum on the operating point of SPM with VDLs. This condition is the theoretical basis of adaptive VFC using SVC. The mathematical equations of SPM and the energy function are described in Appendices A and B respectively. Then, the detail challenges to realize this objective condition are listed. In order to solve these difficulties, we propose two main Theorems and design ASVC-based VFC.

A. Main Results-I: Condition for SLEF

Lemma 1. The equilibrium $\boldsymbol{z_0}$ is the unique globally asymptotically stable point of the structure preserving power systems and the function $E(\boldsymbol{z})$ is an SLEF if:

$$b_{rl} = b_{rl}^* := -\Delta\theta_l M_l, \tag{6}$$

where $M_l = (\nabla_{V_{t_l}} P_{L_l})/V_{t_l}$.

Proof. See the Appendix B. ■

Remark 1. Condition (6) imposes the correlation between reactive power regulation and frequency control by means of the Lyapunov approach. This condition represents the reactive power compensation strategy for the VFC based on the variations of the bus angle difference and the rate of change of active load with respective to the voltage.

Remark 2. As shown in Appendices A and B, the SPM model is only utilized to construct the SLEF and its sufficient condition (6). The considered model does not affect the resulting control scheme, because in the simulations studied in Section IV, all the models used are detailed practical ones.

Based on Lemma 1, the objective of SVC control is to track a desired trajectory b_{rl}^* (to establish convergence of the tracking error $\tilde{b}_{rl} = b_{rl} - b_{rl}^*$ to zero) rendering power systems globally asymptotically stable. The following remarks constitute relevant challenges for the SVC control synthesis:

1. It is difficult to obtain the exact value of active load parameter α_l, because of lack of knowledge of the load model and its time variant features.
2. The reference signal b_{rl}^* to be tracked has uncertainty caused by load parameter α_l.
3. Due to the implicit form of V_{t_l}, the dynamics $\dot{V}_{t_l}$ and $\dot{b}_{rl}^*$ are unknown.

The above challenges are addressed in the next subsections.

Remark 3. Although active load can be modeled as exponential form, for example, $P_{L_l}(V_{t_l}, \alpha_l) = P_{l0}\big(V_{t_l}/V_{t_{l0}}\big)^{\alpha_l}$ such that we have $\alpha_l = \ln(P_{L_l}/P_{l0})/\ln(V_{t_l}/V_{t_{l0}})$, this formulation cannot be used in practice since singular problem will happen when $V_{t_l} = V_{t_{l0}}$. Thus, it is usually difficult to get exact value of unknown load parameter which causes uncertainty in reference signal b_{rl}^*.

Remark 4. In the theoretical derivation, we assume that every VDL bus can be connected by an SVC. However, this does not limit the practicability of the proposed SVC, as shown in the case study, its effectiveness is verified by only installing it on limited load buses.

B. Mathematical Preliminaries

We first introduce the following standard assumptions and useful Lemmas to make the control synthesis tractable.

Assumption 1. There exists unknown positive constant ζ_l, such that $|\dot{V}_{t_l}| < \zeta_l$.

Assumption 2. The unknown load parameter α_l is a slowly time-varying signal, such that $\dot{\alpha}_l \approx 0$.

Lemma 2. For any $\varepsilon > 0$ and $\eta \in \mathbb{R}$, the inequality $0 \leqslant |\eta| - \eta\tanh(\eta/\varepsilon) \leqslant \kappa\varepsilon$ holds, where κ is a constant that satisfies $\kappa = e^{-(\kappa+1)}$, i.e. $\kappa = 0.2785$.

Proof. See reference [22]. ■

Lemma 3. Given a symmetric positive-definite matrix $\boldsymbol{P} \in \mathbb{R}^{q\times q}$ and a differentiable mapping $\boldsymbol{L} : \mathbb{R}^q \longrightarrow \mathbb{R}^q$. If

$$\boldsymbol{P}\nabla_{\boldsymbol{\alpha}}\boldsymbol{L}(\boldsymbol{\alpha}) + [\nabla_{\boldsymbol{\alpha}}\boldsymbol{L}(\boldsymbol{\alpha})]^{\mathrm{T}}\boldsymbol{P} \geqslant 0,\ \forall \boldsymbol{\alpha} \in \mathbb{R}^q, \tag{7}$$

then the following inequality holds

$$(\boldsymbol{a}-\boldsymbol{b})^{\mathrm{T}}\boldsymbol{P}(\boldsymbol{L}(\boldsymbol{a}) - \boldsymbol{L}(\boldsymbol{b})) \geqslant 0,\ \forall \boldsymbol{a}, \boldsymbol{b} \in \mathbb{R}^q. \tag{8}$$

Proof. See reference [23]. ■

C. Main Results-II: ASVC Strategy

We are now ready to state the main results of ASVC.

Theorem 1. Suppose Assumption 1 holds and the real load parameter α_l is known. For system (1), the global tracking between b_{rl} and the reference signal b_{rl}^* can be achieved by the following adaptive controller with four local measurable variables b_{rl}, $\Delta\theta_l$, V_{t_l}, Δf_l for feedback:

$$\begin{aligned} T_{\zeta l}\dot{\hat{\zeta}}_l &= N_l\tilde{b}_{rl}\tanh(N_l\tilde{b}_{rl}/\varepsilon_l), \\ u_l &= -c_l\tilde{b}_{rl} + b_{rl}^* - 2\pi\Delta f_l M_l T_{rl} \\ &\quad - \hat{\zeta}_l N_l\tanh(N_l\tilde{b}_{rl}/\varepsilon_l), \end{aligned} \tag{9}$$

where $\hat{\zeta}_l$ is the estimation of the upper bound ζ_l, $N_l = \Delta\theta_l R_l T_{rl}$, $R_l = (\nabla_{V_{t_l}} P_{L_l})/V_{t_l}^2 - (\nabla^2_{V_{t_l}} P_{L_l})/V_{t_l}$, $T_{\zeta l}$ is the time constant, $c_l > 0$ and $0 < \varepsilon_l < 1$ are the parameters to be tuned.

Proof. See the Appendix C. ■

Theorem 2. Suppose Assumption 2 holds. If there exist a C^1 function $\Theta_l(P_{L_l})$ and a function $\Phi_l(V_{t_l})$ such that

$$\Phi_l \nabla_{\alpha_l} \Theta_l \geqslant 0, \tag{10}$$

then there exists adaptive updating law as

$$T_{\alpha l}\dot{\hat{\alpha}}_l = \Phi_l\big(\Theta_l(P_{L_l}) - \Theta_l\big(P_{L_l}(V_{t_l}, \hat{\alpha}_l)\big)\big), \tag{11}$$

rendering

$$\lim_{t\to\infty} \hat{\alpha}_l = \alpha_l, \tag{12}$$

where $T_{\alpha l}$ is the time constant to be chosen.

Proof. See the Appendix D. ■

Remark 5. Note that our theoretical results are not based on an explicit representation of the load model, one can specify any appropriate load model for the control synthesis. For example, one can choose a monomial with an unknown exponent (see Section III-D).

D. Adaptive SVC Controller Design

Generally speaking, active power load can be modeled as monomial function of the bus voltage magnitude as follows [21] and this model has been widely employed in the literature (for example, [24])

$$P_{L_l}(V_{t_l}, \alpha_l) = P_{l0}(V_{t_l}/V_{t_{l0}})^{\alpha_l}, \tag{13}$$

where P_{l0} represents the active power load at nominal voltage, in pu. For this active load model, P_{l0} and $V_{t_{l0}}$ can be seemed as prior known parameters, but α_l is mostly unknown really and this fact will be considered in the following SVC design process.

For a given load, the active power exponent tends to be constant, at least during a certain period (hours at least). Thus, we propose a load-parametric estimator to solve the first two problems stated in Section III-A. Choose $\Theta_l(P_{L_l}) = P_{L_l}$ and

$$\Phi_l(V_{t_l}) = \begin{cases} 1, & V_{t_l} \geqslant V_{t_{l0}}, \\ -1, & V_{t_l} < V_{t_{l0}}, \end{cases} \tag{14}$$

then we have

$$\Phi_l \nabla_{\alpha_l} \Theta_l = P_{L_l} \left|\ln\left(V_{t_l}/V_{t_{l0}}\right)\right| \geqslant 0,$$

thus the condition (10) holds. By applying Theorem 2 directly, the load-parametric estimator is designed as:

$$T_{\alpha l}\dot{\hat{\alpha}}_l = \Phi_l\big(P_{L_l} - P_{l0}(V_{t_l}/V_{t_{l0}})^{\hat{\alpha}_l}\big). \tag{15}$$

Then, substituting (13) into M_l and R_l, one has $M_l = \alpha_l P_{L_l}/V_{t_l}^2$ and $R_l = \alpha_l(2-\alpha_l)P_{L_l}/V_{t_l}^3$. For simplicity, define two functions of α_l as follows:

$$f_{1l}(\alpha_l) = N_l(\alpha_l)\tilde{b}_{rl}(\alpha_l)\tanh(N_l(\alpha_l)\tilde{b}_{rl}(\alpha_l)/\varepsilon_l),$$

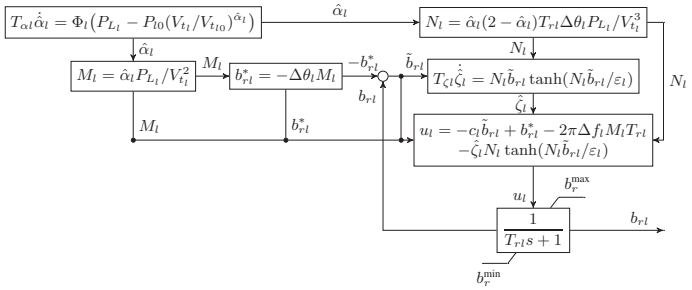

Fig. 2: Block diagram of ASVC.

$$f_{2l}(\alpha_l) = -c_l\tilde{b}_{rl}(\alpha_l) + b^*_{rl}(\alpha_l) - 2\pi\Delta f_l M_l(\alpha_l)T_{rl} - \hat{\zeta}_l N_l(\alpha_l)\tanh(N_l(\alpha_l)\tilde{b}_{rl}(\alpha_l)/\varepsilon_l).$$

Finally, on the basis of Theorem 1, we design practical ASVC control law with only local measurable variables b_{rl}, $\Delta\theta_l$, V_{t_l}, Δf_l, P_{L_l} for feedback as:

$$\begin{aligned} T_{\zeta l}\dot{\hat{\zeta}}_l &= f_{1l}(\hat{\alpha}_l), \\ u_l &= f_{2l}(\hat{\alpha}_l), \end{aligned} \tag{16}$$

eqs. (14) to (16) together constitute the proposed nonlinear ASVC model, its block diagram is also shown in Fig. 2.

Remark 6. The parameter c_l can be chosen depending on the desired goals of the control. To improve the transient performance of bus frequency, we can choose $c_l = c_{l0} + c_{l1}(\Delta f_l)^2$, in which c_{l0} and c_{l1} are positive constants to be tuned. In this way, the controller gain is not remarkably increased since the function $(\Delta f_l)^2$ tends to zero at steady state.

Remark 7. There are five positive parameters $T_{\zeta l}$, $\varepsilon_l(<1)$, c_{l0}, c_{l1} and $T_{\alpha l}$ to be tuned for the ASVC model. It is easy to complete this work. First, both smaller values of $T_{\zeta l}$, ε_l and larger values of c_{l0} and c_{l1} will result in a faster convergence speed. Second, the smaller the value of $T_{\alpha l}$, the less time is spent on the convergence between the load-parametric estimation and the exact value.

IV. Case Study

The case study presented in this section is based on the well-known IEEE New England 39-bus 10-machine system [25]. All dynamic data of this system are provided in [26]. The system includes 10 synchronous machines, 19 loads, 34 transmission lines and 12 transformers. All synchronous generators are equipped with AVRs, power system stabilizers (PSSs) and turbine governors (TGs). The TGs are coordinatd through an automatic generation control. A voltage dependent model is used for representing the loads. With this aim, α_l and β_l denote the power exponents of active and reactive power consumptions, respectively, at bus l.

The complete model of the IEEE 39-bus system used in this section is a set of DAEs (see equation (17)) which include 110 state variables (generators and their regulators) and 220 algebraic variables (voltage magnitudes and angles as well as algebraic variables of the generators and their regulators). Extra variables and equations are included to account for the SVC devices and the phase-locked loop (PLL) required to

TABLE I
PARAMETERS OF DIFFERENT SVC MODELS AND PLL

Name	Values
ASVC	$T_{\zeta l} = 0.01$, $\varepsilon_l = 0.1$, $c_{l0} = 0.01$, $c_{l1} = 25$, $T_{\alpha l} = 0.001$, $T_{rl} = 0.1$, $b_r^{\max} = 1$, $b_r^{\min} = -1$
CSVC	$K_{rl} = 20$, $T_{rl} = 0.01$, $b_r^{\max} = 1$, $b_r^{\min} = -1$ $K_g = 25$, $T_g = 0.01$
PLL	$K_p = 0.1$, $K_i = 0.5$, $T_c = 0.01$

[1] The meanings of parameters K_p, K_i, T_c can be found in [27].

estimate the angle difference $\Delta\theta_l$ and the frequency variation Δf_l signals [27].

It is important to note that, although a lossless transmission system model is adopted for the theoretical derivations and design of the proposed adaptive control, all simulations are actually solved using the detailed transient stability model discussed above, which includes nonlinearities, hard limits and saturations. The simplified model is used because it retains the dynamics that are relevant for the control itself and because analytical Lyapunov energy functions for real-world, lossy transmission networks are not available. Then, the numerical analysis carried out in this section serve to test whether the proposed control is stable when included in the actual system.

The Python-based software DOME [28] is used to implement all the models and solve all simulations presented below.

A. Case Study 1

In this case study, the performances of the proposed ASVC model and extended CSVC model are tested and compared with two scenarios: (a) CSVC ($v_g = 0$) and (b) without SVC. For this purpose, four different tests are considered, the buses 15 and 20 are chosen to be installed by SVCs, and three kinds of SVCs are considered: (i) ASVC; (ii) CSVC; (iii) CSVC+VFC; and (iv) without SVC. Set $\alpha_{15} = 1.15$, $\alpha_{20} = 1.1$, $\beta_{15} = \beta_{20} = 1.8$, and the power exponents of the other load buses are set as 0. The parameters used for different kinds of SVCs are listed in Table I. To ensure that all the tests have same initial operating point, we set $b_{rl}(0) = 0$, i.e., no reactive power is exchanged between the system and the SVCs unless there is a disturbance.

Contingency 1: The test system is simulated through disconnecting the line between buses 16 and 24 and by applying a step increase of the load at bus 15 (3.2 pu to 3.6 pu) at 1 s. To illustrate the effectiveness of the load parametric estimator of ASVC, initial values are provided for $\alpha_{15} = 0.95$ and $\alpha_{20} = 1$. Figure 3 shows that, after applying the disturbance, the load exponents are properly estimated by the proposed adaptive parametric estimator.

The comparative trajectories of the frequency in COI frame and the voltage at bus 15 are shown in Figs. 4-5. Observe that: (i) there is a significant improvement in the system frequency response when using the ASVC; (ii) the CSVC with frequency control also improves the frequency response compared to the cases with CSVC and without SVC; (iii) the ASVC ensures that the post-fault bus voltage is kept within given limits and imposes the lowest voltage and, hence, the lowest power demand; and (iv) using CSVC with and without lag VFC loop,

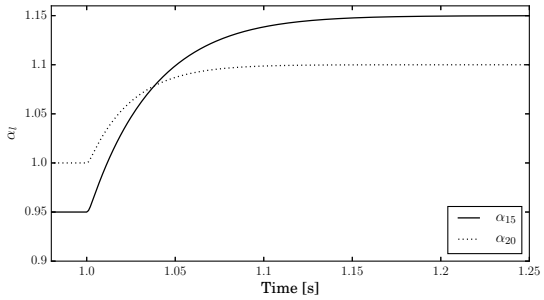

Fig. 3: Estimations of the active power exponents of the VDL at bus 15 and 20.

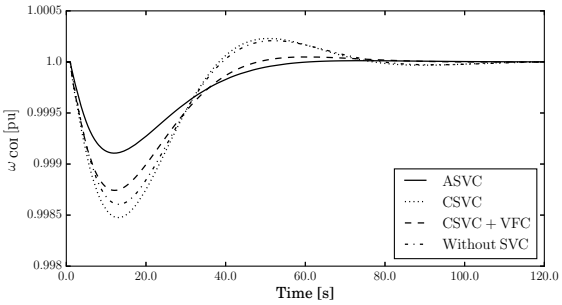

Fig. 4: Response of the frequency in COI frame.

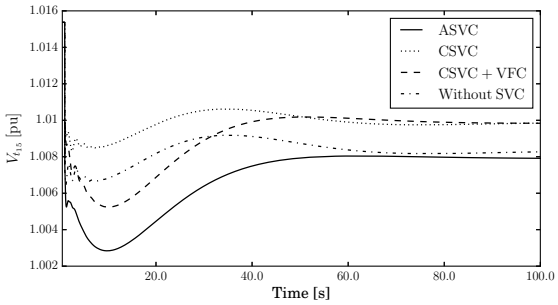

Fig. 5: Response of the voltage at bus 15.

the voltage reaches a steady state operating point close to the reference set point. These results confirm the effectiveness of the proposed nonlinear ASVC that provides overall best dynamic performance.

B. Case Study 2

The previous subsection proves that the ASVC substantially improves the frequency and voltage responses after a relatively low-impact contingency. Next, we compare the impacts of the proposed two SVCs with CSVC on frequency and voltage under relatively large disturbance. With this aim, let buses 3, 4, 7, 15, 20 be installed SVCs. Also the simulation results of the system without SVC are compared. For each load bus l, we set $\alpha_l = 1.3$, $\beta_l = 2$. The parameters used for ASVC and CSVC, and the initialization of SVC are same as in Case Study 1 (see Table I).

Contingency 2: We consider a relatively large disturbance, i.e., the loss of a generation (generating $P_0 = 2.5$ pu) at bus

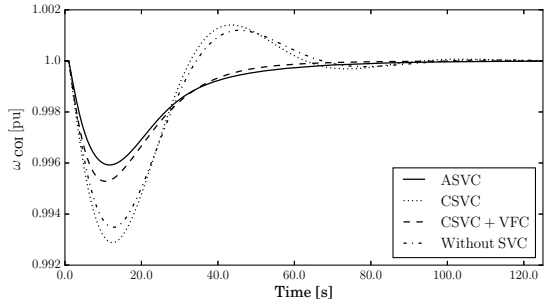

Fig. 6: Response of the frequency in COI frame.

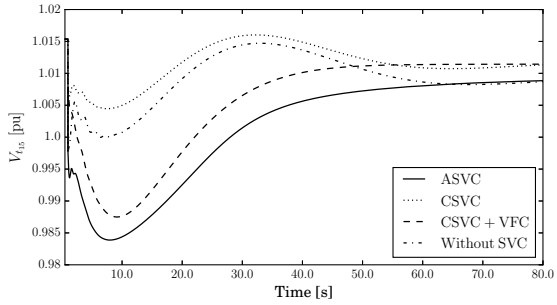

Fig. 7: Response of the voltage at bus 15.

30 at 1 s. The comparative results of the frequency in COI frame and the voltage at bus 15 are shown in Figs. 6-7. The following remarks are relevant: (i) the proposed ASVC leads to the smoothest responses and the best transient performances of system frequency; (ii) ASVC obtains the lowest post-fault bus voltage during the transient and this correspondingly further reduces the power demand; (iii) compared to CSVC and without SVC, the rate of change of frequency is slower using ASVC during the first few seconds of disturbance applied. Consequently, in comparison with CSVC, the proposed ASVC and extended CSVC are more effective to mitigate the effect of large disturbances on bus frequency deviations.

Remark 8. Besides the above mentioned case studies, we have also tried a CSVC+POD test (namely, v_g is chosen as a POD signal). But the result shows that the POD does not contribute in VFC, so this POD test is not described.

V. Conclusion

The paper proposes a nonlinear ASVC controller and an extended CSVC model that improve the dynamic frequency response of multi-machine power systems. The main features of the proposed controller are: (i) it accounts for SPM with nonlinear VDLs; (ii) it requires only local measurements and data without prior knowledge of exact SPM parameters; (iii) it uses five available variables for feedback (see Section III-D); and (iv) it includes only five parameters to be tuned easily (see Remark 7). The results obtained in two cases studies show that the proposed controller outperforms CSVC control schemes on the frequency regulation also in case of large critical disturbances, and it can obtain lower post-fault power demand. Future work will further focus on the analysis of the proposed controller for systems with high penetration of renewable sources.

Appendix A
Structure Preserving Model

colorblack

A. DAE model of Power System

The electromechanical dynamics of synchronous machines are modelled through a transient stability model consisting of a set of nonlinear DAEs as:

$$\begin{aligned} \dot{\boldsymbol{x}} &= \boldsymbol{f}(\boldsymbol{x}, \boldsymbol{y}) \\ \mathbf{0} &= \boldsymbol{g}(\boldsymbol{x}, \boldsymbol{y}) \ , \end{aligned} \tag{17}$$

where $\boldsymbol{x}$ is the vector of state variables of dynamic components (generators, AVRs, PSSs, TGs, SVCs etc); $\boldsymbol{y}$ is the vector of algebraic variables of network (voltage amplitudes and phases of network buses, active and reactive powers, etc.) and dynamic components. These models are described in several book, e.g., [21] and the interested reader is referred to such references for further details.

For the definition of adaptive control, we use a simplified version of (17), which allows the definition of a Lyapunov function and the analytical derivation of the equations of the controller itself. The following models are assumed for the generators, transmission lines, loads and network for the definition of the Lyapunov function utilized in the adaptive control. In the remainder of this appendix, we adopt the following simplified notations:

1. If $l \notin \bar{m}$, then $P_{e_l} = Q_{e_l} = 0$;
2. If $k \notin \Omega_l$, then $B_{lk} = B_{lk}^{sh} = 0$;

where B_{lk} (B_{lk}^{sh}) is (shunt) susceptance of the line between buses l and k, in pu.

B. Generator Model

The jth synchronous machine is modeled by the following usual swing equation where E'_{d_j}, E'_{q_j} are viewed as constants. This common assumption implies on ideal voltage regulation, and has been often adopted in the literature [17], [18], [29].

$$\begin{aligned} \dot{\delta}_j &= \omega_s \omega_j, \\ 2H_j \dot{\omega}_j &= -D_j \omega_j + P_{m_j} - P_{e_j}, \end{aligned} \tag{18}$$

$$\begin{aligned} P_{e_j} &= \frac{E'_{d_j}}{x'_{q_j}} V_{q_j} - \frac{E'_{q_j}}{x'_{d_j}} V_{d_j} - \frac{x'_{dq_j}}{x'_{d_j} x'_{q_j}} V_{d_j} V_{q_j}, \\ Q_{e_j} &= \frac{E'_{d_j}}{x'_{q_j}} V_{d_j} + \frac{E'_{q_j}}{x'_{d_j}} V_{q_j} - \frac{1}{x'_{q_j}} V_{d_j}^2 - \frac{1}{x'_{d_j}} V_{q_j}^2, \end{aligned} \tag{19}$$

where relative angle $\tilde{\delta}_j = \delta_j - \theta_j$, the d- and q-axis components of bus voltage are defined as $V_{d_j} = -V_{t_j} \sin \tilde{\delta}_j$, $V_{q_j} = V_{t_j} \cos \tilde{\delta}_j$, synchronous speed $\omega_s = 2\pi f_0$, in rad/s, H_j is the inertia constant, in s, D_j is the damping coefficient, in pu, P_{m_j} is the mechanical power, in pu, x'_{d_j} (x'_{q_j}) is the d-axis (q-axis) transient reactance of jth machine, in pu, and $x'_{dq_j} = x'_{d_j} - x'_{q_j}$.

C. Lossless Transmission Model

For a multi-machine power network, it has been shown that its lossless characteristic is the basic premise of using the energy function method [30]. This general assumption has been widely used in power systems analysis/control [18], [31]. Only few attempts have been made to remove this constraint and to limited small examples (see, for example, [32]).

Hence, we use a lossless version of transmission line lumped π-circuit as follows [33], [34]:

$$\begin{aligned} P_{lk} &= B_{lk} V_{t_l} V_{t_k} \sin\theta_{lk}, \\ Q_{lk} &= B'_{lk} V_{t_l}^2 - B_{lk} V_{t_l} V_{t_k} \cos\theta_{lk}, \end{aligned} \tag{20}$$

where relative angle $\theta_{lk} = \theta_l - \theta_k$, and $B'_{lk} = B_{lk} - B^{sh}_{lk}$.

D. Load Model

Loads are represented by the following generic C^1 functions of the voltage at the bus l

$$\begin{aligned} P_{L_l} &= P_{L_l}(V_{t_l}, \alpha_l), \\ Q_{L_l} &= Q_{L_l}(V_{t_l}, \beta_l), \end{aligned} \tag{21}$$

where α_l (β_l) is parameter of active (reactive) load model.

E. Network Model

Finally, load power consumption are linked to the grid through well-known power flow equations:

$$\begin{aligned} P_l &:= -P_{e_l} + P_{L_l} + \textstyle\sum_{k=1}^{b} P_{lk} = 0, \\ Q_l &:= (-Q_{e_l} + Q_{L_l} - Q_{rl} + \textstyle\sum_{k=1}^{b} Q_{lk})/V_{t_l} = 0. \end{aligned} \tag{22}$$

Appendix B
Proof of Lemma 1

Proof. First, we consider the following energy function for the SPM with VDLs depicted in Appendix A:

$$\begin{aligned} E(\boldsymbol{z}) = &\sum_{j=1}^{m} \Big(- P_{m_j}\delta_j + \frac{\omega_s H_j}{2}\omega_j^2 \\ &- \frac{E'_{d_j}}{x'_{q_j}} V_{d_j} - \frac{E'_{q_j}}{x'_{d_j}} V_{q_j} + \frac{1}{2x'_{q_j}} V_{d_j}^2 + \frac{1}{2x'_{d_j}} V_{q_j}^2 \Big) \\ &+ \sum_{l=1}^{b}\sum_{k=1}^{b} \Big(\frac{B'_{lk}}{2} V_{t_l}^2 - \frac{B_{lk}}{2} V_{t_l} V_{t_k} \cos\theta_{lk} \Big) \\ &+ \sum_{l=1}^{b} \Big(\Delta\theta_l P_{L_l} + \int_{V_{t_{l0}}}^{V_{t_l}} \frac{Q_{L_l}(z_l)}{z_l} \mathrm{d}z_l \Big). \end{aligned} \tag{23}$$

Under condition (6), partial differentiating E with respect to δ_j, ω_j, V_{t_l} and θ_l respectively yields:

$$\begin{aligned} &\nabla_{\delta_j} E = P_{e_j} - P_{m_j}, \nabla_{\omega_j} E = \omega_s H_j \omega_j, \\ &\nabla_{V_{t_l}} E = Q_l, \nabla_{\theta_l} E = P_l, \end{aligned} \tag{24}$$

which lead to $(\nabla_{\boldsymbol{z}} E)\,|_{\boldsymbol{z}=\boldsymbol{z_0}} = \boldsymbol{0}$.

The Hessian matrix of E is as follows:

$$\mathrm{Hess}(E) = \left[\begin{array}{c:c:cc} \nabla_{\boldsymbol{\delta}} \boldsymbol{P_e} & & \nabla_{\boldsymbol{V}} \boldsymbol{P_e} & \nabla_{\boldsymbol{\theta}} \boldsymbol{P_e} \\ \hdashline & \boldsymbol{H} & & \\ \hdashline \nabla_{\boldsymbol{\delta}} \boldsymbol{Q_f} & & \nabla_{\boldsymbol{V}} \boldsymbol{Q_f} & \nabla_{\boldsymbol{\theta}} \boldsymbol{Q_f} \\ \nabla_{\boldsymbol{\delta}} \boldsymbol{P_f} & & \nabla_{\boldsymbol{V}} \boldsymbol{P_f} & \nabla_{\boldsymbol{\theta}} \boldsymbol{P_f} \end{array}\right], \tag{25}$$

where $\boldsymbol{P_f} = \mathrm{col}(P_l)$, $\boldsymbol{Q_f} = \mathrm{col}(Q_l)$, $\boldsymbol{H} = \mathrm{diag}\{\omega_s H_j\}$.

From the positive definite Jacobian of normal power flow which corresponds to local regularity, and Lemma 1 in [35], one can justify the positive definiteness of $\mathrm{Hess}(E)|_{\boldsymbol{z}=\boldsymbol{z_0}}$. Thus, the energy function $E(\boldsymbol{z})$ has a unique minimum at $\boldsymbol{z} = \boldsymbol{z_0}$. In addition, the time derivative of $E(\boldsymbol{z})$ along the system trajectory is $\dot{E} = -\omega_s \sum_{j=1}^{m} D_j \omega_j^2$.

Therefore, $E(\boldsymbol{z})$ is an SLEF and the structure preserving power systems are globally asymptotically stable under condition (6). ■

Appendix C
Proof of Theorem 1

Proof. Note $\Delta\dot{\theta}_l = 2\pi\Delta f_l$ such that

$$\dot{b}^*_{rl} = -2\pi\Delta f_l M_l + \Delta\theta_l R_l \dot{V}_{t_l}. \tag{26}$$

For simplicity, denote $\tilde{\zeta}_l = \hat{\zeta}_l - \zeta_l$ as the parameter estimation error. Then, differentiating the Lyapunov function $W_1 = \frac{1}{2}\sum_{l=1}^{b}(T_{rl}\tilde{b}_{rl}^2 + T_{\zeta l}\tilde{\zeta}_l^2)$ with respect to time yields:

$$\begin{aligned} \dot{W}_1 = &\textstyle\sum_{l=1}^{b} \Big(- (1+c_l)\tilde{b}_{rl}^2 + \tilde{b}_{rl}(u_l + c_l\tilde{b}_{rl} - b^*_{rl} \\ &+ 2\pi\Delta f_l M_l T_{rl} + \hat{\zeta}_l N_l \tanh(N_l\tilde{b}_{rl}/\varepsilon_l)) \\ &+ \tilde{\zeta}_l(T_{\zeta l}\dot{\hat{\zeta}}_l - N_l\tilde{b}_{rl}\tanh(N_l\tilde{b}_{rl}/\varepsilon_l)) \\ &- \dot{V}_{t_l} N_l \tilde{b}_{rl} - \zeta_l N_l \tilde{b}_{rl}\tanh(N_l\tilde{b}_{rl}/\varepsilon_l)\Big). \end{aligned} \tag{27}$$

By substituting (9) into (27) and using Lemma 2, we get:

$$\begin{aligned} \dot{W}_1 &< \textstyle\sum_{l=1}^{b} \Big(- (1+c_l)\tilde{b}_{rl}^2 \\ &\qquad + \zeta_l\big(|N_l\tilde{b}_{rl}| - N_l\tilde{b}_{rl}\tanh(N_l\tilde{b}_{rl}/\varepsilon_l)\big)\Big) \\ &\leqslant \textstyle\sum_{l=1}^{b} \Big(- (1+c_l)\tilde{b}_{rl}^2 + \kappa\varepsilon_l\zeta_l\Big). \end{aligned} \tag{28}$$

Therefore, it is clear the global tracking problem of system (1) can be achieved by employing the adaptive controller (9) with small enough designed parameter ε_l. ■

Appendix D
Proof of Theorem 2

Proof. Define $\tilde{\alpha}_l = \hat{\alpha}_l - \alpha_l$ and let $W_3 = \frac{T_{\alpha l}}{2}\tilde{\alpha}_l^2$, $\gamma_l(\alpha_l) = \Phi_l(V_{t_l})\Theta_l\big(P_{L_l}(V_{t_l}, \alpha_l)\big)$. Differentiating W_3 along the trajectory of system (11) yields

$$\dot{W}_3 = (\hat{\alpha}_l - \alpha_l)\big(\gamma_l(\alpha_l) - \gamma_l(\hat{\alpha}_l)\big). \tag{29}$$

Under condition (10), we get $\nabla_{\alpha_l}\gamma_l(\alpha_l) \geqslant 0$. Using Lemma 3, we have $\dot{W}_3 \leqslant 0$ which implies $\lim_{t\to\infty}\hat{\alpha}_l = \alpha_l$. ■

References

[1] P. Tielens and D. Van Hertem, "The relevance of inertia in power systems," *Renewable and Sustainable Energy Reviews*, vol. 55, pp. 999–1009, 2016.

[2] B. Kroposki, B. Johnson, Y. Zhang, V. Gevorgian, P. Denholm, B.-M. Hodge, and B. Hannegan, "Achieving a 100% renewable grid: Operating electric power systems with extremely high levels of variable renewable energy," *IEEE Power and Energy Magazine*, vol. 15, no. 2, pp. 61–73, 2017.

[3] F. Milano, F. Dörfler, G. Hug, D. J. Hill, and G. Verbič, "Foundations and challenges of low-inertia systems," in *20th Power System Computation Conference (PSCC)*, Dublin, Ireland, 2018, pp. 1–25.

[4] M. Cheng, J. Wu, S. J. Galsworthy, C. E. Ugalde-Loo, N. Gargov, W. W. Hung, and N. Jenkins, "Power system frequency response from the control of bitumen tanks," *IEEE Transactions on Power Systems*, vol. 31, no. 3, pp. 1769–1778, May 2016.

[5] I. Beil, I. Hiskens, and S. Backhaus, "Frequency regulation from commercial building HVAC demand response," *Proceedings of the IEEE*, vol. 104, no. 4, pp. 745–757, April 2016.

[6] E. Vrettos, C. Ziras, and G. Andersson, "Fast and reliable primary frequency reserves from refrigerators with decentralized stochastic control," *IEEE Transactions on Power Systems*, vol. 32, no. 4, pp. 2924–2941, July 2017.

[7] A. Moeini and I. Kamwa, "Analytical concepts for reactive power based primary frequency control in power systems," *IEEE Transactions on Power Systems*, vol. 31, no. 6, pp. 4217–4230, Nov 2016.

[8] A. Ballanti, L. N. Ochoa, K. Bailey, and S. Cox, "Unlocking new sources of flexibility: Class: The world's largest voltage-led load-management project," *IEEE Power and Energy Magazine*, vol. 15, no. 3, pp. 52–63, 2017.

[9] D. Chakravorty, B. Chaudhuri, and S. Y. R. Hui, "Estimation of aggregate reserve with point-of-load voltage control," *IEEE Transactions on Smart Grid*, vol. 9, no. 5, pp. 4649–4658, Sept 2018.

[10] M. Farrokhabadi, C. A. Cañizares, and K. Bhattacharya, "Frequency control in isolated/islanded microgrids through voltage regulation," *IEEE Transactions on Smart Grid*, vol. 8, no. 3, pp. 1185–1194, 2017.

[11] Z. Wang and J. Wang, "Review on implementation and assessment of conservation voltage reduction," *IEEE Transactions on Power Systems*, vol. 29, no. 3, pp. 1306–1315, May 2014.

[12] M. T. Holmberg, M. Lahtinen, J. McDowall, and T. Larsson, "SVC Light® with energy storage for frequency regulation," in *IEEE Conference on Innovative Technologies for an Efficient and Reliable Electricity Supply*, 2010, pp. 317–324.

[13] A. El-Emary and M. El-Shibina, "Application of static var compensation for load frequency control," *Electric machines and power systems*, vol. 25, no. 9, pp. 1009–1022, 1997.

[14] H. Ayres, I. Kopcak, M. Castro, F. Milano, and V. Da Costa, "A didactic procedure for designing power oscillation dampers of FACTS devices," *Simulation Modelling Practice and Theory*, vol. 18, no. 6, pp. 896–909, 2010.

[15] ABB FACTS Division, "A matter of facts deliver more high quality power," ABB, Product Guide, 2015.

[16] G. De Carne, G. Buticchi, M. Liserre, and C. Vournas, "Load control using sensitivity identification by means of smart transformer," *IEEE Transactions on Smart Grid*, vol. 9, no. 4, pp. 2606–2615, July 2018.

[17] D. J. Hill and C. N. Chong, "Lyapunov functions of Lur'e-Postnikov form for structure preserving models of power systems," *Automatica*, vol. 25, no. 3, pp. 453–460, 1989.

[18] T. L. Vu and K. Turitsyn, "Lyapunov functions family approach to transient stability assessment," *IEEE Transactions on Power Systems*, vol. 31, no. 2, pp. 1269–1277, 2016.

[19] D. Swaroop, J. K. Hedrick, P. P. Yip, and J. C. Gerdes, "Dynamic surface control for a class of nonlinear systems," *IEEE Transactions on Automatic Control*, vol. 45, no. 10, pp. 1893–1899, 2000.

[20] Q. Gong and C. Qian, "Global practical tracking of a class of nonlinear systems by output feedback," *Automatica*, vol. 43, no. 1, pp. 184–189, 2007.

[21] F. Milano, *Power system modelling and scripting*. Springer Science & Business Media, 2010.

[22] M. M. Polycarpou and P. A. Ioannou, "A robust adaptive nonlinear control design," *Automatica*, vol. 32, no. 3, pp. 423–427, 1996.

[23] X. Liu, R. Ortega, H. Su, and J. Chu, "Immersion and Invariance adaptive control of nonlinearly parameterized nonlinear systems," *IEEE Transactions on Automatic Control*, vol. 55, no. 9, pp. 2209–2214, 2010.

[24] A. Ballanti and L. F. Ochoa, "Voltage-Led load management in whole distribution networks," *IEEE Transactions on Power Systems*, vol. 33, no. 2, pp. 1544–1554, 2018.

[25] Á. Ortega and F. Milano, "Comparison of bus frequency estimators for power system transient stability analysis," in *2016 IEEE International Conference on Power System Technology (POWERCON)*, Sept 2016, pp. 1–6.

[26] Illinois Center for a Smarter Electric Grid, "IEEE 39-Bus System."

[27] A. Cataliotti, V. Cosentino, and S. Nuccio, "A phase-locked loop for the synchronization of power quality instruments in the presence of stationary and transient disturbances," *IEEE Transactions on Instrumentation and Measurement*, vol. 56, no. 6, pp. 2232–2239, 2007.

[28] F. Milano, "A python-based software tool for power system analysis," in *IEEE PES General Meeting*, Vancouver, BC, 2013, pp. 1–5.

[29] T. L. Vu and K. Turitsyn, "A framework for robust assessment of power grid stability and resiliency," *IEEE Transactions on Automatic Control*, vol. 62, no. 3, pp. 1165–1177, 2017.

[30] N. Narasimhamurthi, "On the existence of energy function for power systems with transmission losses," *IEEE Transactions on Circuits & Systems*, vol. 31, no. 2, pp. 199–203, 1984.

[31] S. Mehraeen, S. Jagannathan, and M. L. Crow, "Power system stabilization using adaptive neural network-based dynamic surface control," *IEEE Transactions on Power Systems*, vol. 26, no. 2, pp. 669–680, 2011.

[32] M. Anghel, F. Milano, and A. Papachristodoulou, "Algorithmic construction of Lyapunov functions for power system stability analysis," *IEEE Transactions on Circuits and Systems-I: Regular Papers*, vol. 60, no. 9, pp. 2533–2546, 2013.

[33] W. Dib, A. E. Barabanov, R. Ortega, and F. Lamnabhi-Lagarrigue, "An explicit solution of the power balance equations of structure preserving power system models," *IEEE Transactions on Power Systems*, vol. 24, no. 2, pp. 759–765, 2009.

[34] K. R. Padiyar, *Structure preserving energy functions in power systems: theory and applications*. CRC Press, 2013.

[35] B. He, X. Zhang, and X. Zhao, "Transient stabilization of structure preserving power systems with excitation control via energy-shaping," *International Journal of Electrical Power & Energy Systems*, vol. 29, no. 10, pp. 822–830, 2007.

Yong Wan was born in Liaoning, China, in 1985. He received the B.E. degree from Nanjing Normal University, China, in 2008, and the M.E. and Ph.D. degrees from Northeastern University, China, in 2010 and 2013 respectively, all in Automatic Control. In 2014, he joined College of Automation Engineering in Nanjing University of Aeronautics and Astronautics, China, where he is currently a lecturer. His research interests include power system control and stability, nonlinear adaptive control.

Mohammed Ahsan Adib Murad (S'18) received B.Sc. degree in electrical engineering from Islamic University of Technology, Bangladesh in 2009, and double M.Sc. degree in Smart Electrical Networks and Systems from KU Leuven, Belgium and KTH, Sweden in 2015. He is currently pursuing the PhD degree with the department of electrical and electronic engineering, University College Dublin, Ireland. His current research interests include power system modeling and dynamic analysis.

Muyang Liu (S'17) received from University College Dublin, Ireland, the ME in Electrical Energy Engineering in 2016. Since September 2016, she is a Ph.D. candidate with University College Dublin. Her scholarship is funded through the SFI Investigator Award with title "Advanced Modelling for Power System Analysis and Simulation". Her current research interests include stability analysis and robust control of power system with inclusion of measurement delays.

Federico Milano (S'02, M'04, SM'09, F'16) received from the Univ. of Genoa, Italy, the ME and Ph.D. in Electrical Eng. in 1999 and 2003, respectively. From 2001 to 2002 he was with the Univ. of Waterloo, Canada, as a Visiting Scholar. From 2003 to 2013, he was with the Univ. of Castilla-La Mancha, Spain. In 2013, he joined the Univ. College Dublin, Ireland, where he is currently Professor of Power Systems Control and Protections. His research interests include power system modelling, control and stability analysis.